THE JOURNAL OF BIOLOGICAL CHEMISTRY VOL. 290, NO. 48, pp. 28834–28846, November 27, 2015

A Novel α2/α4 Subtype-selective Positive Allosteric Modulator of Nicotinic Acetylcholine Receptors Acting from the C-tail of an α Subunit*

Received for publication, July 8, 2015, and in revised form, September 22, 2015 Published, JBC Papers in Press, October 2, 2015, DOI 10.1074/jbc.M115.676551

Jingyi Wang[‡], Alexander Kuryatov[‡], Zhuang Jin[§], Jack Norleans[‡], Theodore M. Kamenecka[§], Paul J. Kenny[¶], and Jon Lindstrom[‡1]

From the [‡]Department of Neuroscience, Perelman School of Medicine at the University of Pennsylvania, Philadelphia, Pennsylvania 19104, [§]Department of Molecular Therapeutics, Scripps Research Institute, Scripps, Florida 33458, and [¶]Department of Pharmacology and Systems Therapeutics, Icahn School of Medicine at Mount Sinai, New York, New York 10029

Background: Nicotinic acetylcholine receptors (nAChRs) are involved in nicotine addiction and some neurological disorders.
Results: A novel positive allosteric modulator potentiates activation through the C-tail of one α4 subunit but requires two α4 to reactivate desensitized nAChRs.
Conclusion: Higher occupancy in allosteric sites promotes nAChR opening and alleviates desensitization.
Significance: These α4 modulators may be useful for basic and clinical applications.

Positive allosteric modulators (PAMs) of nicotinic acetylcholine receptors (nAChR) are important therapeutic candidates as well as valuable research tools. We identified a novel type II PAM, (*R*)-7-bromo-*N*-(piperidin-3-yl)benzo[*b*]thiophene-2-carboxamide (Br-PBTC), which both increases activation and reactivates desensitized nAChRs. This compound increases acetylcholine-evoked responses of α2* and α4* nAChRs but is without effect on α3* or α6* nAChRs (* indicates the presence of other nAChR subunits). Br-BPTC acts from the C-terminal extracellular sequences of α4 subunits, which is also a PAM site for steroid hormone estrogens such as 17β-estradiol. Br-PBTC is much more potent than estrogens. Like 17β-estradiol, the non-steroid Br-PBTC only requires one α4 subunit to potentiate nAChR function, and its potentiation is stronger with more α4 subunits. This feature enables Br-BPTC to potentiate activation of (α4β2)(α6β2)β3 but not $(\alpha6\beta2)_2\beta3$ nAChRs. Therefore, this compound is potentially useful *in vivo* for determining functions of different α6* nAChR subtypes. Besides activation, Br-BPTC affects desensitization of nAChRs induced by sustained exposure to agonists. After minutes of exposure to agonists, Br-PBTC reactivated short term desensitized nAChRs that have at least two α4 subunits but not those with only one. Three α4 subunits were required for Br-BPTC to reactivate long term desensitized nAChRs. These data suggest that higher PAM occupancy promotes channel opening more efficiently and overcomes short and long term desensitization. This C-terminal extracellular domain could be a target for developing subtype or state-selective drugs for nAChRs.

Nicotinic acetylcholine receptors (nAChRs)[2] are critical for nicotine addiction and important for several neuropsychiatric disorders (1–3). They are ligand-gated ion channels formed from five homologous subunits whose subtypes are defined by their subunit composition. There are 12 neuronal types of subunits: α2–10 and β2–4. Homomeric nAChRs like α7 assemble from only α7 subunits, whereas heteromeric nAChRs usually require both α and β subunits (4, 5). Both homomeric and heteromeric nAChRs form orthosteric agonist binding sites at interfaces between the subunits in the extracellular domain. Recently, various ligands have been identified that activate, inhibit, or potentiate activation of nAChRs from allosteric sites other than the agonist binding sites (4, 6, 7). These include positive allosteric modulators (PAMs), negative allosteric modulators, and allosteric agonists (6, 8, 9). These drugs bind to various places in nAChRs, including the extracellular domain, transmembrane domain, and the extracellular C terminus (*e.g.* C-tail) (6, 7). There are interests in developing PAMs because agonists both activate and desensitize nAChRs and because subtype selectivity is hard to achieve with agonists due to similarity between ACh binding in different nAChR subtypes. By contrast, PAMs enhance nAChR function in an activity-dependent manner, potentially modulating the endogenous pattern of signaling rather than constantly activating or desensitizing nAChRs. PAMs also increase the potential for subtype specificity. This is because diversity of PAM binding sites in nAChRs provides better chances to develop selective therapeutics than does targeting the relatively similar ACh binding sites.

Based on pharmacology, there are two types of PAMs (10). Type I PAMs increase peak responses. Type II PAMs not only increase peak responses but also the duration of channel opening by delaying desensitization. This makes type II PAMs espe-

* This work was supported by National Institute on Drug Abuse Grant DA030929. The authors declare that they have no conflicts of interest with the contents of this article.
[1] To whom correspondence should be addressed: Dept. of Neuroscience, Perelman School of Medicine of the University of Pennsylvania, 130A John Morgan, Philadelphia, PA 19104-6074. Tel.: 215-573-2859; Fax: 215-573-2858; E-mail: JSLKK@mail.med.upenn.edu.

[2] The abbreviations used are: nAChR, nicotinic acetylcholine receptor; ACh, acetylcholine; Br-PBTC, (*R*)-7-bromo-*N*-(piperidin-3-yl)benzo[*b*]thiophene-2-carboxamide; DHβE, dihydro-β-erythroidine hydrobromide; PAM, positive allosteric modulator.

cially efficacious. In some cases they can act as allosteric agonists (8). Understanding the pharmacology and potentiation mechanism of PAMs should facilitate design of more potent and selective modulators. There is no direct correlation between where a PAM binds and which type of PAM it is (6). Some PAMs bind in the transmembrane domain near the gate for the cation channel whose opening they influence (6). These transmembrane PAMs can be either type I or type II. Here we describe a novel type II PAM, Br-PBTC,[3] which acts from the C-tail of the α4 subunit. Discovering how this site, which is distant from both agonist binding sites and the channel gate, influences activation and desensitization should provide new insights on the structure and function of nAChRs.

Higher occupancy of agonist sites increases activation and speed of desensitization of both heteromeric and homomeric nAChRs (11–13). Knowledge of how binding of PAMs affects activation and desensitization is limited. Some estrogens act as PAMs through the C-tail of α4 (14). Their PAM effect increases with the number of α4 subunits with free C-tails in a nAChR (15). By contrast, Br-PBTC potentiates α4 concatemers and free α4 subunits. Using this novel PAM and various concatemers, we investigated how PAM site occupancy influences activation and desensitization of nAChRs expressed in *Xenopus* oocytes and mammalian cell lines. We found that occupying one PAM site is sufficient to potentiate nAChR activation, and higher PAM site occupancy promotes nAChR opening and alleviates short and long term desensitization more efficiently. This C-tail potentiation mechanism might be applicable to other nAChR subtypes and facilitate development of other subtype-selective drugs.

Experimental Procedures

Chemicals—Methodology for preparing reactants for synthesizing Br-PBTC is described as follows.

Ethyl 7-Bromobenzo[b]thiophene-2-carboxylate—3-Bromo-2-fluorobenzaldehyde (406.0 mg, 2.0 mmol), ethyl mercaptoacetate (242 μl, 2.2 mmol), triethylamine (556 μl, 4.0 mmol), and acetonitrile (10 ml) were added to a 50-ml round-bottom flask and stirred at 60 °C overnight. The acetonitrile was removed *in vacuo*, and the residue was dissolved in ethyl acetate (30 ml) and water (10 ml). The layers were separated, and the aqueous layer was extracted with ethyl acetate (2×). The combined organics were dried ($MgSO_4$) and concentrated to give the title compound (538 mg, 95%). ^{1}H NMR ($CDCl_3$, 400 MHz) δ 8.15 (s, 1H), 7.84 (d, 1H, J = 8.0 Hz), 7.61 (d, 1H, J = 7.6 Hz), 7.31 (t, 1H, J = 7.6 Hz), 4.43 (q, 2H, J = 6.8 Hz), 1.46 (t, 3H, J = 6.8 Hz).

7-Bromobenzo[b]thiophene-2-carboxylic Acid—Ethyl 7-bromobenzo[b]thiophene-2-carboxylate (500.0 mg, 1.7 mmol), lithium hydroxide (250.0 mg, 10.4 mmol), tetrahydrofuran (6 ml), and water (8 ml) were added to a 50-ml round-bottom flask and stirred at room temperature until the starting material was consumed as judged by thin layer chromatography analysis. The majority of the tetrahydrofuran was removed *in vacuo*. The resulting crude mixture was acidified with aqueous hydrochloric acid (~pH = 3) and cooled in an ice bath. The solids were filtered and washed with cold water (about 6 ml) to give the title compound (392 mg, 90%).

Synthesis of Br-PBTC—A mixture of 7-bromobenzo[b]thiophene-2-carboxylic acid (25.6 mg, 0.1 mmol), (*R*)-*tert*-butyl 3-aminopiperidine-1-carboxylate (24.0 mg, 0.12 mmol), *N*,*N*-diisopropylethylamine (52 μl, 0.3 mmol), and 1-[bis(dimethylamino)methylene]-1H-1,2,3-triazolo[4,5-b]pyridinium 3-oxid hexafluorophosphate (57.0 mg, 0.15 mmol) in dimethylformamide (2 ml) was stirred at room temperature for 12 h. The reaction mixture was diluted with ethyl acetate (15 ml) and washed with water (4 ml, 3×). The organic layer was dried ($MgSO_4$) and concentrated *in vacuo*. The crude residue was dissolved in CH_2Cl_2 (5 ml), trifluoroacetic acid (TFA) (5 ml) was added, and the reaction was stirred at room temperature for 1 h. The reaction was concentrated *in vacuo* to give a crude product, which was purified by reverse-phase preparative HPLC (A: methanol and acetonitrile (1:1, v/v); B: water containing TFA (0.1%, v/v)). The title compound was obtained as the TFA salt (31.6 mg, 70%). ^{1}H NMR (CD_3OD, 400 MHz) δ 8.10 (s, 1H), 7.90 (dd, 1H, *J* = 0.8, 8.0 Hz), 7.63 (dd, 1H, *J* = 0.8, 7.6 Hz), 7.36 (t, 1H, *J* = 8.0 Hz), 4.11 (m, 1H), 3.34 (m, 1H), 3.13 (m, 1H), 2.74 (m, 2H), 2.08 (m, 1H), 1.69 (m, 2H). LC/MS (ESI) 339, 341 (M+H). A 10 mM stock of Br-PBTC was prepared in dimethyl sulfoxide. Dilutions of drugs were prepared daily in testing buffer before use. All other chemicals were purchased from Sigma unless otherwise noted.

cDNAs and cRNAs—Human α2, α3, α4, α6, β2, and β4 were cloned in this laboratory (13, 16–19). Concatemers were formed by linking the C terminus of one subunit to the N terminus of the next. The trimeric concatemer β2$(QAP)_n$α4$(QAP)_n$β2 (abbreviated as β2-α4-β2) was synthesized through linking together β2$(QAP)_n$α4 with QAP linker and β2. β2$(QAP)_n$α4 was made similarly as β3$(QAP)_n$α6, which was described (20). A BspEI site was introduced at the end of the mature peptide of β2 using a CCCAGCTCCAAGTCCGGACCTTCCTCATCTC oligonucleotide. The $(QAP)_n$ linker was then inserted between the BspEI site at the end of β2 and the FspI site at the beginning of α4. At the end of the coding domain of α4 in the β2QAPα4 dimer we introduced a AgeI site (GCTGGCTGGCATGATCACCGGTGGGACCGGGGAGCCTG oligonucleotide), which is complementary to the XmaI site of the second $(QAP)_n$ linker in the concatemer β2$(QAP)_n$α4$(QAP)_n$β2. The second $(QAP)_n$ linker was prepared from the β2$(QAP)_n$α4 piece. We mutated the FspI site at the beginning of the α4 sequence into a BstBI site. The second $(QAP)_n$ linker with new restriction sites was cut out using XmaI site and BstBI enzymes. We introduced a BstBI restriction site at the beginning of the mature peptide of β2 using a GGCATGATCTTCGAAACGGATACAGAGGAG oligonucleotide. These allowed us to link together the β2QAPα4 dimer with the AgeI site, the QAP linker with XmaI and BstBI ends, and the β2 subunits with the BstBI restriction site at the beginning of mature peptide. The resulting construct was recloned into the pBS SK(−) vector using the EcoRI restriction enzyme. The resulting clone linearized with EcoRV for expression in oocytes. Syntheses of tetrameric and pentameric concatemers (*i.e.* β2-α4-β2-α4 and β3-α6-β2-α4-β2) was described (21, 22).

[3] A provisional patent for Br-PBTC and its analogues has been applied for through the Scripps Research Institute with the authors (T. M. Kamenecka, P. J. Kenny, J. M. Lindstrom, J. Wang, Z. Jin, and C. Doebelin).

Four of the five chimeras of α3 and α4 subunits were prepared previously (23). Chimeras were numbered according to the amino acid sequences of the mature subunit. $\alpha3^{(1-440)}/\alpha4^{(561-594)}$ was prepared by ligating three pieces of DNA: a 0.6-kb fragment from the NcoI to BstEII site of the α3 subunit, a 1-kb fragment from the HidIII to BstEII site of the α3 subunit, and a 3.1-kb fragment from the NcoI to HidIII site of the α4 subunit in the pSP64 vector. The ligation mixture was transformed into XL10-Gold ultracompetent cells (Stratagene, La Jolla, CA), and the right clone was chosen from a restriction enzyme digest.

A C-tail mutant (noted as $\alpha4^{AAC}$) was obtained by mutating the last four amino acids of the α4 subunit, alanine-glycine-methionine-isoleucine, to alanine-alanine-cysteine followed by a stop codon. Mutations were introduced using the PfuUltra high-fidelity DNA polymerase (Agilent, Santa Clara, CA) following the manufacturer's instructions. All mutations were confirmed by sequencing.

After linearization and purification of cDNAs, cRNA transcripts were prepared *in vitro* using mMessage mMachine kits (Ambion, Austin, TX). Concentrations of cDNAs and cRNAs were calculated by spectrophotometry.

Cell Culture and Transfection—All cells were maintained as described previously (17). The human embryonic kidney tsA201 (HEK) cell lines stably expressing human α4β2, α4β4, α2β2, α2β4, α3β2, and α3β4 were described (13). The α4β2 cell line expresses a mixture of $(\alpha4\beta2)_2\alpha4$ and $(\alpha4\beta2)_2\beta2$ nAChRs (24). HEK cells that express only one stoichiometry, either $(\alpha4\beta2)_2\alpha4$ or $(\alpha4\beta2)_2\beta2$, were obtained by transfecting a dimeric concatemer $\beta2(QAP)_n\alpha4$ cell line with α4 or β2 subunits.[4]

FLEXstation Experiments—For functional tests of nAChRs expressed in HEK cells, we used a FLEXstation (Molecular Devices, Sunnyvale, CA) bench-top scanning fluorometer as described by Kuryatov *et al.* (25). To increase the expression level of α2β3, α3β2, and $(\alpha4\beta2)_2\beta2$ nAChRs, the plates were incubated at 29 °C for 20 h before being tested. A membrane potential fluorescent indicator kit (Molecular Devices) was used according to the manufacturer's protocols. In PAM experiments, serial dilutions of Br-PBTC were manually added to the assay plate 15 min before the addition of agonists during recording unless otherwise noted. In short term desensitization experiments, 6 min after agonists were added to cell culture wells, Br-PBTC or dihydro-β-erythroidine hydrobromide (DHβE) was automatically added into the wells during recording. In long term desensitization experiments, nicotine or DHβE was incubated with cells for 6 h before recording. Br-PBTC with or without DHβE was added to the cell culture wells during recording. Each data point was averaged from three to four responses from separate wells. The potency and maximum efficacy of drugs were calculated by fitting the Hill equation to the concentration/response relationship using a nonlinear least squares curve fitting method (Kaleidagraph; Abelbeck/Synergy, Reading, PA): $I(x) = I_{max}\,[x^{n}{}_{H}/(x^{n}{}_{H} + EC_{50}{}^{n}{}_{H})]$, where $I(x)$ is the peak current measured at the drug concentration x, I_{max} is the maximum current peak at the saturating concentration, EC_{50} is the drug concentration required to achieve half of the maximum response, and n_H is the Hill coefficient.

Ooctye Removal and Injection—Oocytes were removed surgically from *Xenopus laevis* and defolliculated as described (13, 18).

Oocyte injections were performed within 48 h after surgery. Oocytes were injected with 20–40 ng of concatemer cRNA and free single subunit at a 1:1 ratio. A total of 2–20 ng of cRNA was injected for free wild type or chimeric α and β subunits at a 4:1 ratio to force expression of the $(\alpha)_3(\beta2)_2$ stoichiometry or at 1:4 ratio to force expression of the $(\alpha)_2(\beta)_3$ stoichiometry. To express homomeric α7 nAChRs, 70 ng of cRNA was injected to each oocyte. The function was assayed 3–7 days after injection.

Electrophysiology—Currents in oocytes were measured using the OpusXpress 6000A (Molecular Devices, Union City, CA), an automated two-electrode voltage clamp amplifier that enables recording up to eight oocytes in parallel (13). Oocytes were voltage-clamped at a holding potential of −50 mV. 200 μl of drugs were delivered on top of oocytes for 4 s (s) through the sidewall of the bath to minimize disturbance to oocytes. Between drug applications, oocytes received a 30-s prewash and 223-s post-wash of ND96 solution (96 mM NaCl, 2 mM KCl, 1.8 mM $CaCl_2$, 1 mM $MgCl_2$, 5 mM HEPES, pH 7.6) with 0.5 μM atropine perfused through the bath at a rate of 3 ml/min unless otherwise noted.

Peak amplitudes of experimental responses were calculated relative to ACh responses to normalize the data and compensate for variable expression levels among oocytes. The PAM effect of Br-PBTC was calculated by comparing increased responses with Br-PBTC relative to responses to ACh alone. Mean and S.E. were calculated from normalized responses. Statistical analyses were performed using Student's *t* test. More than four oocytes were tested for each experiment.

Pre-application of Br-PBTC gave slightly higher PAM effects on wild type and chimeric nAChRs than co-application with agonists. But conclusions were the same for both application methods. To save time, we thereafter used the co-application method to evaluate the PAM effects in experiments performed in oocytes. In short term desensitization experiments, 1 mM ACh was applied to oocytes for 4 s at the rate of 3 ml/min followed by another 56 s at 0.75 ml/min. Then the oocytes were incubated for an additional 5 min in a static bath before a co-application with 1 mM ACh plus 3 μM Br-PBTC for 4 s at 3 ml/min. Control experiments were performed on the same oocytes before Br-PBTC applications following the same protocol in which 3 μM Br-PBTC was replaced with 0.1% (v/v) DMSO. Reactivation by Br-PBTC was calculated by normalizing the response of 3 μM Br-PBTC to the response of ACh applied before Br-PBTC. In antagonist inhibition experiments, α-conotoxin MII was applied for 4 s at the rate of 3 ml/min followed by another 56 s at 0.75 ml/min. To fully block ACh activation, the oocytes were then incubated for an additional 16 min in a static bath before co-application of ACh (3 μM) or ACh together with Br-PBTC (3 μM).

[4] A. Kuryatov, J. Wang, and J. Lindstrom, manuscript in preparation.

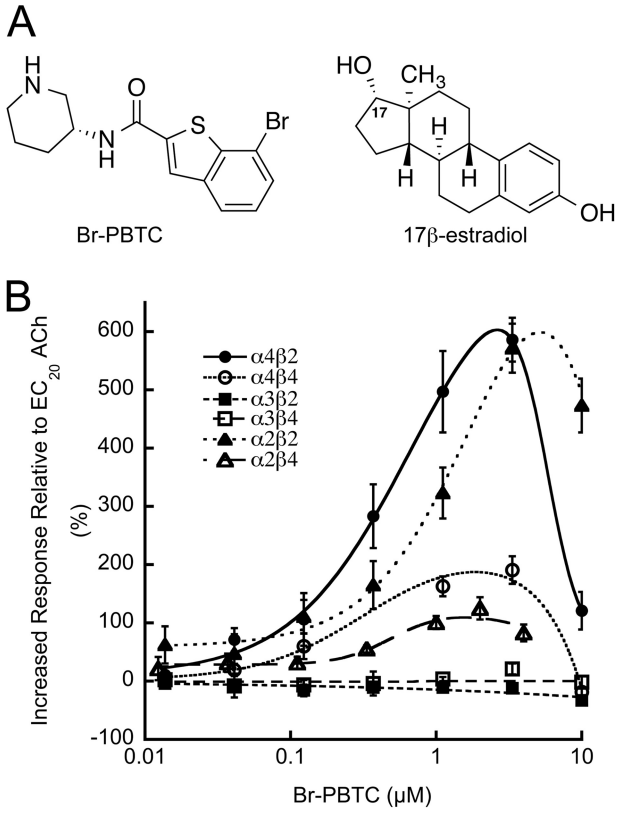

FIGURE 1. **Chemical structure and nAChR subtype selectivity of the PAM Br-PBTC.** *A*, structural comparison of Br-PBTC and 17β-estradiol. *B*, concentration/response curves of Br-PBTC for potentiating activation of nAChR subtypes expressed in HEK cell lines. Various concentrations of Br-PBTC were pre-applied for 15 min before acute application of ACh at EC_{20} concentrations (*i.e.* α4β2, 0.4 μM; α4β4, 1 μM; α3β2, 4 μM; α3β4, 5 μM; α2β2, 0.4 μM; α2β4, 0.8 μM). Potentiation effects were calculated by increased peak responses by Br-PBTC relative to responses evoked by ACh. Results are the mean ± S.E. (*error bars*).

Results

Br-PBTC Selectively Affects α2 and α4 Subunits—To investigate the subtype selectivity of compound Br-PBTC (Fig. 1*A*), we tested its ability to potentiate ACh activation of various subtypes of nAChRs stably expressed in HEK cells (Fig. 1*B*). Br-PBTC increased the activation by EC_{20} ACh of α2- and α4-containing nAChRs by 119–560% (Table 1). EC_{50} values for Br-PBTC ranged from 0.261 to 0.660 μM (Table 1), equal to the most potent nAChR PAMs (6, 7). At >3 μM, Br-PBTC inhibited its own potentiation effect, perhaps because it behaved as an open channel blocker like some other nAChR PAMs and ACh itself (26). Br-PBTC did not alter activation by ACh of α3β2 or α3β4 nAChRs (Fig. 1*B*). We also evaluated the effect of Br-PBTC (up to 3 μM) on activation on homomeric α7 nAChRs expressed in *Xenopus* oocytes. The maximum increased peak response by Br-PBTC was 33.9 ± 33.8%. Because the potentiation is small with large error and only appeared at 1 μM Br-PBTC, we do not think that Br-PBTC potentiates activation of α7 nAChRs. Br-PBTC did not activate these heteromeric or homomeric nAChR subtypes by itself (data not shown). Therefore, Br-PBTC is an α2 and α4 nAChR subtype-selective PAM.

Br-PBTC potentiated activation of β2-containing nAChRs more than β4-containing nAChRs. The relatively higher efficacy of Br-PBTC on α2β2 and α4β2 nAChRs could result from Br-PBTC having greater effects on the $(\alpha\beta)_2\alpha$ stoichiometry or from the preference of Br-PBTC for β2 over β4. Our α4β4 nAChR cell line expresses both $(\alpha4\beta4)_2\beta4$ and $(\alpha4\beta4)_2\alpha4$ stoichiometries (13). To express fixed stoichiometries of α4β2 and α4β4, we transiently overexpressed one subunit over the other in oocytes. We used 3 μM Br-PBTC to study its potentiation effects on activation of $(\alpha4\beta2)_2\alpha4$, $(\alpha4\beta2)_2\beta2$, $(\alpha4\beta4)_2\alpha4$, and $(\alpha4\beta4)_2\beta4$ by various concentrations of ACh (Fig. 2). Br-PBTC has a greater effect on β2* than β4* nAChRs with the same stoichiometry. It increased maximum ACh efficacy of the $(\alpha4\beta2)_2\alpha4$ by 6.8 ± 2.2-fold, larger than the 1.7 ± 0.1-fold increase on $(\alpha4\beta4)_2\alpha4$ nAChRs. Br-BPTC increased activation of $(\alpha4\beta2)_2\beta2$ but showed no effect on $(\alpha4\beta4)_2\beta4$. However, Br-PBTC did potentiate the activation of the $(\alpha2\beta4)_2\beta4$ stoichiometry as evidenced by its action on our α2β4 cell line, which only expresses this stoichiometry (13). Therefore, Br-PBTC potentiates activation of both $(\alpha\beta)_2\alpha$ and $(\alpha\beta)_2\beta$ stoichiometries but has a weaker effect on β4-containing than β2-containing nAChRs.

TABLE 1
Potencies and maximum efficacies of potentiation by Br-PBTC on activation by EC_{20-30} ACh
nAChR subtypes were expressed in HEK cell lines. ND refers to data not detected when the PAM effects were too small to obtain meaningful potency and efficacy values.

nAChR subtypes	Br-PBTC EC_{50}	n_{Hill}	I_{max}
	μM		%
α2β2	0.660 ± 0.377	1.07 ± 0.47	560 ± 102
α2β4	0.286 ± 0.039	1.10 ± 0.09	202 ± 7
α3β2	ND	ND	<0
α3β4	ND	ND	<21
α4β2	0.446 ± 0.086	1.16 ± 0.17	651 ± 47
α4β4	0.237 ± 0.340	0.770 ± 0.552	119 ± 45
$(\alpha4\beta2)_2\alpha4$	0.165 ± 0.033	1.67 ± 0.47	246 ± 17
$(\alpha4\beta2)_2\beta2$	0.275 ± 0.100	1.17 ± 0.40	101 ± 10

Br-PBTC increased the maximum ACh efficacy of the two stoichiometries of α4β2 greatly in oocytes (Fig. 2). We investigated whether Br-PBTC potentiates activation of nAChRs with defined stoichiometries expressed in HEK cell lines. The defined stoichiometries were obtained by expressing a β2-α4 concatemer with a free α4 or β2 subunit (Fig. 3*A*). These cell lines also allowed us to study the effect of Br-PBTC on long term desensitized nAChRs, which is described in later sections. Br-PBTC enhanced activation by EC_{40-50} ACh of both stoichiometries. It is 2.5-fold more efficacious at activation of the $(\alpha4\beta2)_2\alpha4$ stoichiometry by EC_{40-50} ACh (Fig. 3*A*). But its potentiation efficacies evaluated by ACh at EC_{100} are similar between the two stoichiometries (Fig. 3, *B* and *C*). The potencies of Br-PBTC are similar for the two stoichiometries, at ~200 nM (Table 1). $(\alpha4\beta2)_2\beta2$ nAChRs have two high ACh sensitivity sites each at α4/β2 interfaces. $(\alpha4\beta2)_2\alpha4$ nAChRs have these two high sensitivity sites and a third low ACh sensitivity site at the α4/α4 interface (27, 28). The different potentiation effects evaluated by medium and maximal concentrations of ACh could result from different effects of Br-PBTC on sensitivity of nAChRs. The ACh concentration/response curve of $(\alpha4\beta2)_2\alpha4$ nAChRs in the absence of Br-PBTC contains two components representing the high affinity α4/β2 agonist sites ($EC_{50}1$ = 0.220 ± 0.056 μM) and the low affinity α4/α4 site ($EC_{50}2$ = 18.1 ± 5.7 μM) in this nAChR subtype. In the pres-

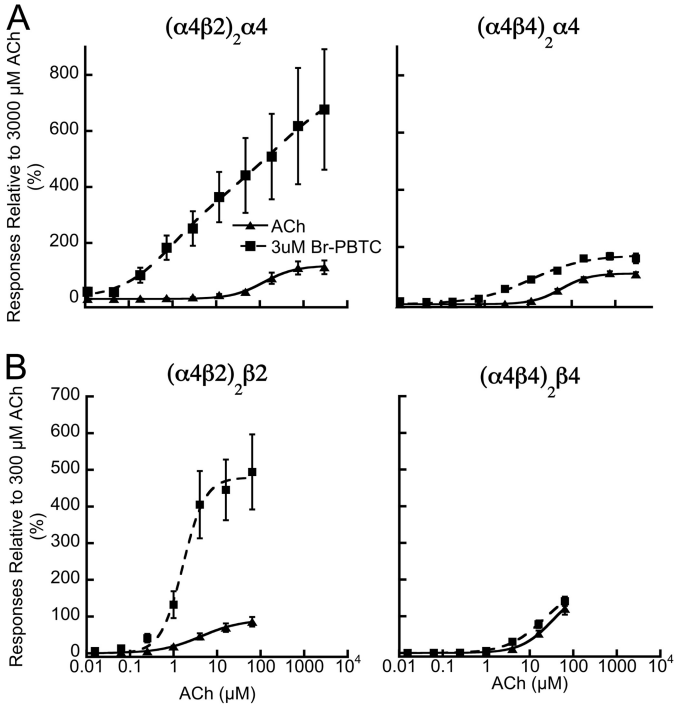

FIGURE 2. **Br-PBTC potentiates both β2- and β4- containing nAChRs but with a greater effect on β2* nAChRs.** Free α4 subunits were expressed with β2 or β4 subunit in oocytes at ratios of 5:1 or 1:5. This enables expression of one desired stoichiometry at a time. *A*, Br-PBTC (3 μM) potentiates activation of both $(\alpha4\beta2)_2\alpha4$ and $(\alpha4\beta4)_2\alpha4$ nAChRs by various concentrations of ACh. *B*, Br-PBTC (3 μM) potentiates activation of $(\alpha4\beta2)_2\beta2$ but not that of $(\alpha4\beta4)_2\beta4$ nAChRs.

ence of Br-PBTC, the ACh concentration/response curve became monophasic with $EC_{50} = 0.0481 \pm 0.0043$ μM (Fig. 3*B* and Table 2). Therefore, Br-PBTC has a much higher effect on activation of $(\alpha4\beta2)_2\alpha4$ nAChRs by EC_{40-50} ACh than by EC_{100} ACh. Conversely, Br-PBTC had little effect on the potency of $(\alpha4\beta2)_2\beta2$ nAChRs, EC_{50} (without Br-PBTC) $= 0.992 \pm 0.193$ μM, and EC_{50} (with Br-PBTC) $= 0.429 \pm 0.079$ μM (Table 2). Therefore, Br-PBTC has a lower efficacy on activation of $(\alpha4\beta2)2\beta2$ than $(\alpha4\beta2)2\alpha4$ nAChRs when evaluated by EC_{40-50} ACh.

Two effects might account for the difference of potency changes by Br-PBTC on the two stoichiometries; 1) Br-PBTC requires the three α4 subunits to affect agonist affinity, or 2) Br-PBTC increases agonist affinity to the low ACh affinity α/α site but does not affect the high ACh affinity α/β sites. To test these hypotheses, we expressed β2-α4-β2-α4 concatemers with α3 subunits in oocytes to obtain $(\alpha4\beta2)_2\alpha3$, which has two α4β2 binding sites like $(\alpha4\beta2)_2\beta2$ and an additional low ACh affinity α3α4 site very similar to the α4/α4 agonist site (13). In parallel, we also expressed $(\alpha4\beta2)_2\alpha4$ and $(\alpha4\beta2)_2\beta2$ in oocytes. The Br-PBTC potentiation effects on ACh efficacy were greater in oocytes than in HEK cells (Table 2). This could be because the Br-PBTC potentiated activation by the high concentration of ACh reached the detection limit of the membrane potential dye that is used to assay HEK cells or because the different lipid environment between HEK cells and oocyte affected conformational change induced by Br-PBTC. However, Br-PBTC potentiation effects on ACh potencies of $(\alpha4\beta2)_2\alpha4$ and $(\alpha4\beta2)_2\beta2$ were similar on oocytes and HEK cells. Br-PBTC increased the sensitivity of $(\alpha4\beta2)_2\alpha4$ to ACh by 37-fold but had a minimal effect on the sensitivities of $(\alpha4\beta2)_2\alpha3$ and $(\alpha4\beta2)_2\beta2$ (Table 2). This suggests that three α4 subunits are required for Br-PBTC to increase agonist sensitivity of nAChRs.

In summary, Br-PBTC is an α2/α4 subtype-selective PAM. It increases potencies of nAChRs with three α4 subunits and efficacies of nAChRs with two or three α4 subunits. Its potentiation effect is larger on β2-containing than β4-containing nAChRs. The following pharmacology study mainly focused on α4β2* nAChRs, which are the most prevalent nAChRs in brain.

Br-PBTC Potentiates Activation from the Extracellular C-terminal Domain of α4 Subunits—Because Br-PBTC has no effect on α3* nAChRs, we expressed various chimeras of α3 and α4 subunits in *Xenopus* oocytes to identify the Br-PBTC potentiation site in the α4 subunit. Fig. 4 illustrates the chimeras of α3 and α4 used. Because Br-PBTC potentiates activation of ACh more strongly at intermediate agonist concentrations, we used ACh at EC_{30-40} to test the PAM effects of Br-PBTC on α3β2, α4β2, and their chimeras (Fig. 5*A*). Br-PBTC could not activate nAChRs by itself but increased ACh activation of α4β2 nAChRs expressed in oocytes by 385 ± 61% (Fig. 5). Similar to the HEK cell results, Br-BPTC did not potentiate α3β2 nAChRs expressed in oocytes. Chimeras $\alpha4^{(1-207)}/\alpha3^{(208-446)}$ and $\alpha4^{(1-297)}/\alpha3^{(298-446)}$, which have the α3 cytoplasmic, M4, and C-tails, abolished potentiation by Br-PBTC. Chimeras retaining α4 sequences in these domains, $\alpha3^{(1-207)}/\alpha4^{(208-594)}$ and $\alpha3^{(1-297)}/\alpha4^{(298-594)}$, exhibited Br-PBTC potentiation. In the chimera $\alpha3^{(1-440)}/\alpha4^{(561-594)}$, Br-PBTC PAM effects resembled wild type α4 subunit (Fig. 5). These data suggest that Br-PBTC potentiates from the region M4 to the C terminus and is likely to bind in or close to this region. The C-tail of human α4 binds to endogenous steroids such as 17β-estradiol (14, 29). To test whether Br-PBTC binds to the α4 subunit C-tail, we mutated the last four amino acids of human α4 subunit (AGMI) to alanine-alanine-cysteine, noted as $\alpha4^{AAC}$. This AAC sequence corresponds to the C-tail of the rat α4 subunit and when substituted for the last four amino acids of human α4 abolished potentiation by 17β-estradiol (14). This mutant decreased potentiation by Br-PBTC to 70 ± 18% ($p < 0.01$ compared with wild type; Fig. 5). Attenuation instead of elimination of the Br-PBTC PAM effect by this C-tail mutant suggests that Br-PBTC binds to the C-tail but closer to the M4 domain than does 17β-estradiol. Both the AAC mutation and an additional tryptophan to leucine mutation before the AGMI sequence are required to abolish potentiation by an ethynyl derivative of 17β-estradiol (14). This tryptophan may help retain the PAM effect of Br-BPTC via cation-π interaction between the tryptophan side chain and the secondary amine of Br-PBTC.

Br-PBTC Potentiates nAChRs through a Single α4 Subunit—PAM efficacy of 17β-estradiol increases with more free α4 C-tails in a nAChR (15). Because Br-PBTC also binds to this C-tail site, we investigated the effect of the number of α4 subunits on the potentiation profile of Br-PBTC. Br-PBTC does not affect functions of α3* nAChRs; thus, we expressed the free α3 subunit with various concatemers of α4 and β2 subunits in *Xenopus* oocytes to decrease the numbers of Br-PBTC potentiation sites in a nAChR (Fig. 6*A*). Another benefit of using α3 to

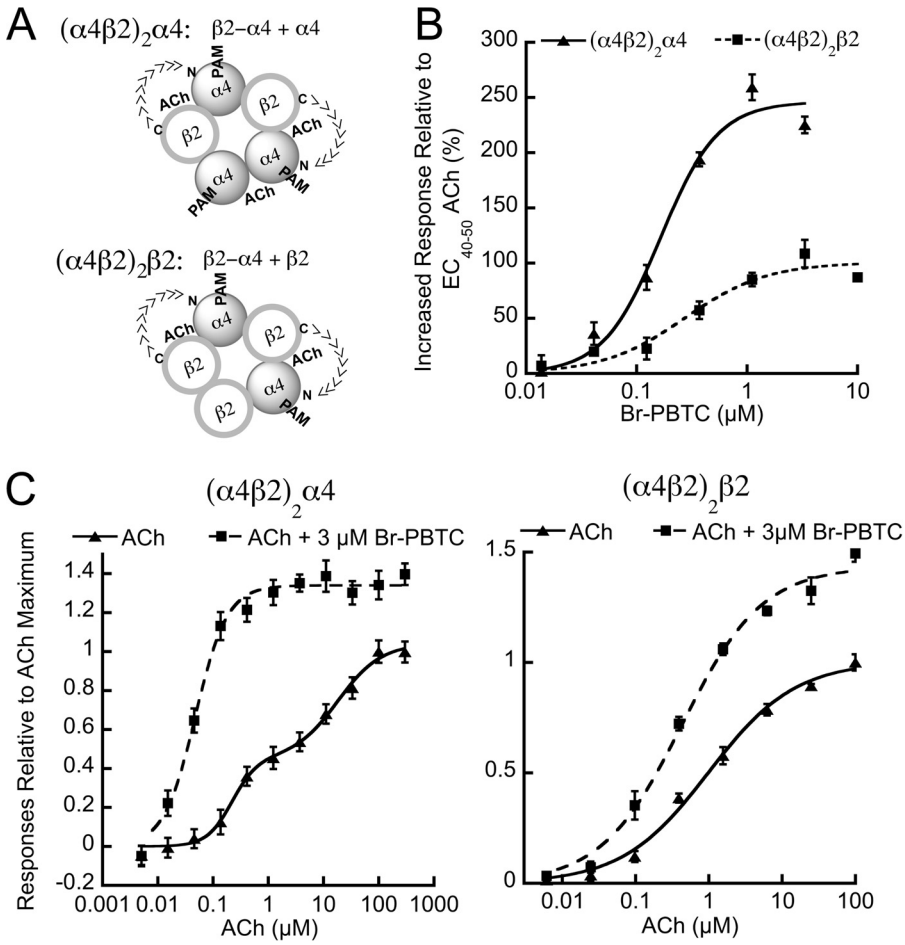

FIGURE 3. **Br-PBTC potentiates activation of both stoichiometries of α4β2 nAChRs.** Concatemeric nAChRs of defined stoichiometries were expressed in HEK cell lines. *A*, illustration of these nAChRs expressed from β2-α4 concatemers in combination with free α4 or β2 subunits. ACh indicates ACh binding sites at subunit interfaces. *PAM* indicates PAM binding sites near α4 C-tails. *B*, concentration/response curves for Br-PBTC potentiation of EC_{40-50} ACh. Various concentrations of Br-PBTC were pre-applied to HEK cells for 15 min before acute application of ACh at EC_{40-50} (3 μM for $(\alpha4\beta2)_2\alpha4$ and 0.4 μM for $(\alpha4\beta2)_2\beta2$ nAChRs). *C*, potentiation by 3 μM Br-PBTC of ACh activation of $(\alpha4\beta2)_2\alpha4$ and $(\alpha4\beta2)_2\beta2$ nAChRs. Results are the mean ± S.E. (*error bars*).

TABLE 2

Effect of 3 μM Br-PBTC on potencies and efficacies of ACh to activate nAChRs

ACh concentration/response curves were determined on oocytes or HEK cell lines expressing defined stoichiometries. The maximum efficacy was defined as 100% for ACh without PAMs. In oocytes, defined stoichiometries were obtained by injecting β2-α4-β2-α4 concatemers with a free subunit. Each data point was collected from more than four oocytes or more than three wells of cells. The $(\alpha4\beta2)_2\alpha4$ cell line exhibits a two-component concentration/response curve due to a high sensitivity component reflecting its two α4/β2 ACh binding sites and a low affinity component reflecting activation in combination with the low sensitivity α4/α4 site. The concentration/response data for $(\alpha4\beta2)_2\alpha4$ obtained from oocytes were too noisy to fit a biphasic curve, so were approximated with a monophasic curve.

nAChR subtypes	Drug	ACh EC_{50}		n_{Hill}	I_{max}
			μM		%
Assays in HEK cell lines					
$(\alpha4\beta2)_2\alpha4$	ACh alone	High affinity	0.220 ± 0.056	1.91 ± 0.62	100
		Low affinity	18.1 ± 5.7	1.11 ± 0.42	
	+Br-PBTC		0.0481 ± 0.0043	1.51 ± 0.18	134 ± 2
$(\alpha4\beta2)_2\beta2$	ACh alone		0.992 ± 0.193	0.735 ± 0.080	100
	+Br-PBTC		0.429 ± 0.079	0.790 ± 0.094	143 ± 5
Assays in oocytes					
$(\alpha4\beta2)_2\alpha4$	ACh alone[a]		108 ± 45	0.762 ± 0.126	100
	+Br-PBTC		2.89 ± 1.38	0.478 ± 0.080	418 ± 31
$(\alpha4\beta2)_2\beta2$	ACh alone[a]		1.02 ± 0.10	0.959 ± 0.114	100
	+Br-PBTC		2.02 ± 0.16	0.988 ± 0.063	712 ± 120
$(\alpha4\beta2)_2\alpha3$	ACh alone[a]		101 ± 20	0.977 ± 0.141	100
	+Br-PBTC		37.8 ± 8.6	0.597 ± 0.053	352 ± 15

[a] Data reported previously (13).

replace the α4 subunit is that then these nAChRs have the same numbers of agonist binding sites. They all have at least one high ACh affinity α4/β2 site. A low affinity ACh site can be formed at α4/α4 and α3/α4 interfaces (13, 27, 28). $(\alpha3\beta4)_2\alpha3$ nAChRs showed lower ACh sensitivity than $(\alpha3\beta4)_2\alpha4$ nAChRs (30). Therefore, a low affinity ACh site is likely to be present at the α3/α3 interface.

We tested the effect of 3 μM Br-PBTC on peak currents evoked by ACh, a feature shared by both type I and type II PAMs (Fig. 6*B*). This concentration is enough to evoke a max-

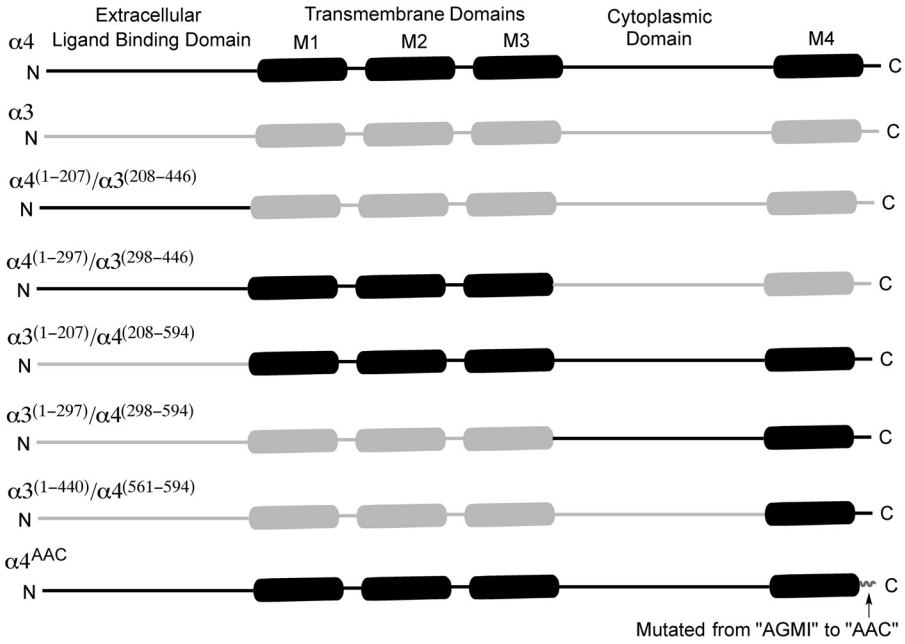

FIGURE 4. **Schematic illustration of human nAChR α3 and α4 subunit chimeras.** The α3 sequences are *gray*, and the α4 sequences are *black*. $\alpha4^{AAC}$ is an α4 subunit with its last four amino acids replaced with alanine-alanine-cysteine. These were chosen because this mutation inhibits the PAM effect of 17β-estradiol. This modified C-tail is annotated as a *gray squiggly line*.

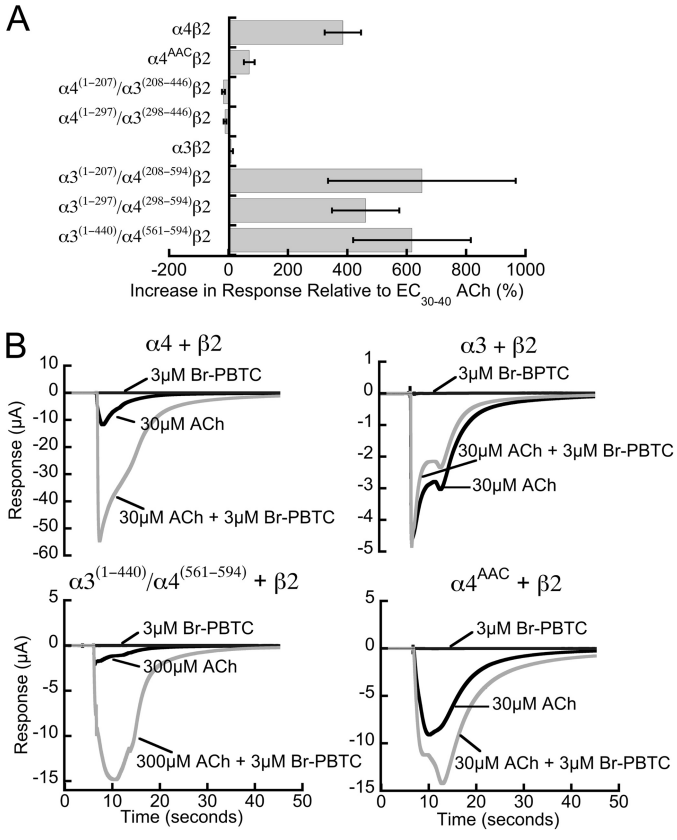

FIGURE 5. **Summary of potentiation effects of Br-PBTC on α3/α4 nAChR chimeras expressed in oocytes.** Br-PBTC (3 μM) was co-applied with EC_{30-40} ACh to each oocyte. Each data point was collected from more than four oocytes. *A*, *bar graph* comparison of the PAM effects of Br-PBTC. *B*, representative response kinetics for wild type α3β2, α4β2, $\alpha4^{AAC}\beta2$, and $\alpha3^{(1-440)}/\alpha4^{(561-594)}\beta2$ nAChRs. Results are the mean ± S.E. (*error bars*).

imal PAM effect for nAChRs containing two or three α4 subunits (Fig. 3*A*). Br-PBTC potentiated activation of $(\alpha4\beta2)_2\alpha4$ nAChRs expressed from the β2-α4-β2-α4 concatemer and free α4 similarly to those expressed from only free subunits (Figs. 5*A* and 6). This is different from estrogens, which do not potentiate concatemers in which the α4 subunit C-tail is linked to another subunit such as α4-β2 (29, 31). Therefore, the concatemer linker has no effect on potentiation by Br-PBTC. Br-PBTC increased activation of nAChRs by both medium (100 μM) and maximal (3000 μM) concentrations of ACh as long as there was more than one α4 subunit (Fig. 6*B*). This is consistent with the property of 17-β estradiol, another known C-tail binding PAM (15). Moreover, the potentiation effect of $(\alpha4\beta2)_2\alpha3$ nAChRs with two α4 subunits was larger, and the effect on $(\alpha4\beta2)_2\alpha4$ with three α4 subunits was the largest. These data suggest that higher PAM occupancy increases the efficiency of channel opening.

Br-PBTC can increase channel activation by a maximal concentration of ACh. This is similar to what was observed with α4β2 nAChRs expressed in HEK cells (Fig. 3*B*). At higher concentrations of agonists, nAChRs desensitize more rapidly. The potentiation by Br-PBTC on 3000 μM ACh could be due to increasing channel conductance or increased open state probability or destabilizing or slowing entry into the desensitized state.

Br-PBTC Can Reactivate Both Short Term and Long Term Desensitized nAChRs—To investigate whether Br-PBTC affects channel desensitization, we applied 1000 μM ACh for 6 min to oocytes expressing α4* nAChRs to desensitize nAChRs before acute application of Br-PBTC (3 μM) with ACh (1000 μM) (Fig. 7). Representative response kinetics are shown in Fig. 7*B*. Most of the nAChRs were desensitized after 6 min of incubation with ACh. Br-PBTC reactivated both $(\alpha4\beta2)_2\alpha4$ and $(\alpha4\beta2)_2\alpha3$, but

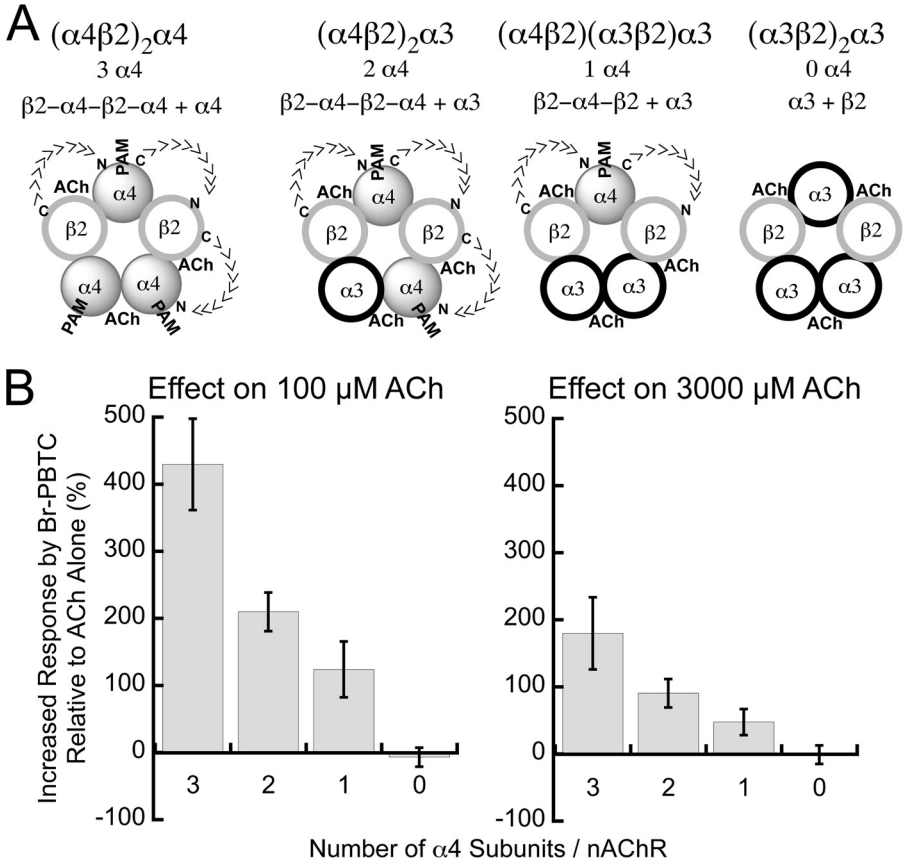

FIGURE 6. **Br-PBTC PAM effect increases with the number of α4 subunits in a nAChR.** Each data point was collected from more than five oocytes. *A*, illustration of nAChRs constructs used that contain different numbers of α4 subunits. *B*, potentiation by Br-PBTC (3 μM) increases with the number of α4 subunits in a nAChR. Br-PBTC was co-applied with 100 or 3000 μM ACh. Results are the mean ± S.E. (*error bars*).

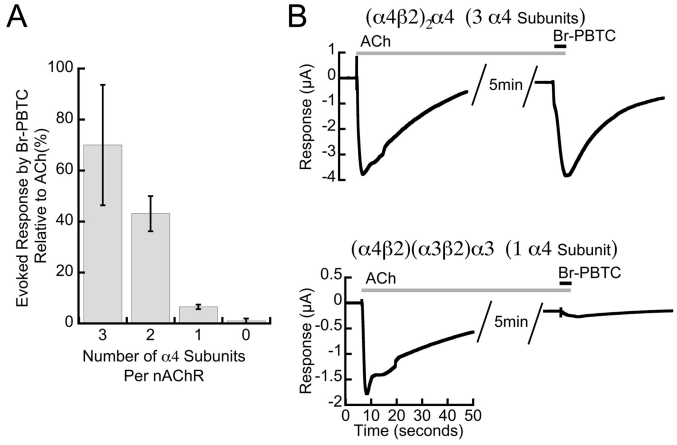

FIGURE 7. **Br-PBTC reactivates short term desensitized nAChRs expressed in oocytes.** To desensitize nAChRs, ACh (1000 μM) was applied to oocytes for 6 min before its co-application with Br-PBTC (3 μM). Each data point was collected from more than five oocytes. *A*, Br-PBTC requires two or more α4 subunits to reactivate short term desensitized nAChRs. The efficacy of reactivation increases with more α4 subunits in a nAChR. *B*, response kinetics from representative oocytes. Results are the mean ± S.E. (error bars).

it had little effect on $(\alpha4\beta2)(\alpha3\beta2)\alpha3$ nAChRs. This suggests that this type II effect requires binding to two or more α4 subunits. This type II property of Br-PBTC was also observed in mammalian HEK cells that express $(\alpha4\beta2)_2\alpha4$ or $(\alpha4\beta2)_2\beta2$ nAChRs (Fig. 8). Br-PBTC reactivated nAChRs desensitized by either ACh or nicotine for 6 min. We use a membrane potential fluorescent indicator to assay nAChR responses in HEK cells. This method is not as sensitive to the kinetics of channel function as the two-electrode voltage clamp method performed on oocytes. Therefore, we did not observe a higher PAM effect on desensitized $(\alpha4\beta2)_2\alpha4$ than $(\alpha4\beta2)_2\beta2$ (Fig. 8), as we expected from oocyte experiments (Fig. 7). Another factor contributing to this discrepancy is that because $(\alpha4\beta2)_2\beta2$ desensitizes slower than $(\alpha4\beta2)_2\alpha4$, more $(\alpha4\beta2)_2\beta2$ nAChRs were still in the open state (represented by the portion blocked by DHβE applied alone in Fig. 8) when Br-PBTC was applied. This was not the case for the experiments we performed on α4* nAChRs expressed in oocytes (Fig. 7).

Unlike ACh, which is quickly hydrolyzed by esterase, nicotine can persist in brains for hours (32). This causes long term desensitization of nAChRs in smokers. Because Br-PBTC can reactivate short term desensitized nAChRs with more than two α4 subunits (Figs. 7 and 8), we studied its effect on nAChRs expressed in HEK cells after 6 h of exposure to 0.5 μM nicotine (Fig. 9). This concentration of nicotine is found in smokers (32). After 6 h with nicotine, nAChRs were all desensitized because application of DHβE to these nAChRs showed no blockage of activation (*black traces* in Fig. 9, *A* and *B*). Interestingly, Br-PBTC (4 μM) efficiently reactivated nicotine long term desensitized $(\alpha4\beta2)_2\alpha4$ nAChRs but only weakly reactivated desensitized $(\alpha4\beta2)_2\beta2$ nAChRs (Fig. 9, *A* and *B*). The desensitized $(\alpha4\beta2)_2\beta2$ could be less sensitive to reactivation by Br-PBTC. Therefore, we determined the dependence on Br-BPTC concentration of reactivation of desensitized nAChRs (Fig. 9*C*).

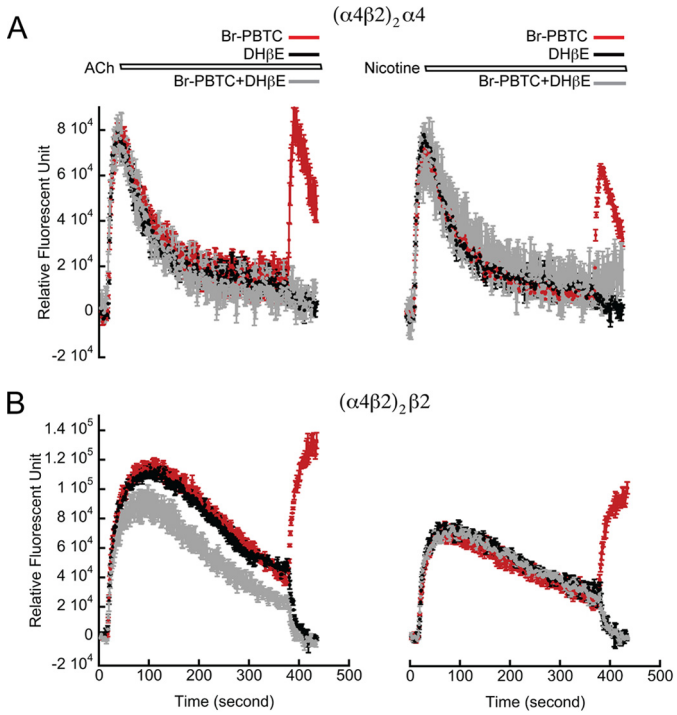

FIGURE 8. **Br-PBTC reactivates short term desensitized $(\alpha4\beta2)_2\alpha4$ and $(\alpha4\beta2)_2\beta2$ nAChRs expressed in HEK cells.** Saturating concentrations of agonists were added to desensitize nAChRs. Because of the low ACh affinity site at the α4/α4 interface, higher concentrations of agonists were used for $(\alpha4\beta2)_2\alpha4$ than $(\alpha4\beta2)_2\beta2$. Br-PBTC (3 μM) and DHβE (1 μM) were added separately or together to nAChRs 6 min after addition of agonist. The antagonist DHβE prevents activation. *A*, ACh (300 μM) and nicotine (100 μM) desensitized $(\alpha4\beta2)_2\alpha4$ nAChRs. *B*, ACh (100 μM) and nicotine (10 μM) desensitized $(\alpha4\beta2)_2\beta2$ nAChRs. Results are the mean ± S.E. (*error bars*).

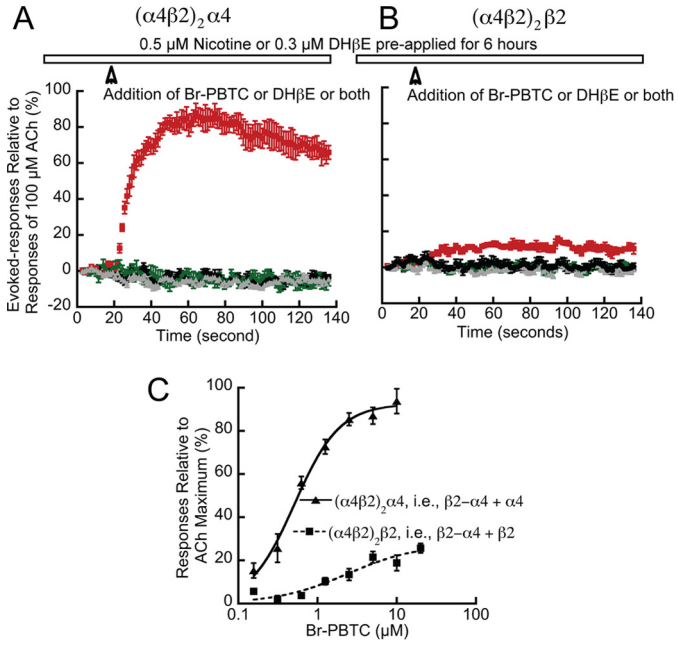

FIGURE 9. **Br-PBTC reactivates long term desensitized nAChRs.** HEK cell lines expressing fixed stoichiometries were used (*i.e.* β2-α4 concatemers plus free α4 or β2 subunits). Nicotine (0.5 μM) or DHβE (0.3 μM) was preincubated with cell culture wells for 6 h before recording. Br-PBTC (4 μM) and/or DHβE (1 μM) were added at 20 s. Response kinetics are displayed for Br-PBTC applied to nicotine (*red*) or DHβE (*green*) treated nAChRs. Nicotine completely desensitized $(\alpha4\beta2)_2\alpha4$ nAChRs after 6 h as the addition of DHβE showed no effect (*black*). *A*, Br-PBTC reactivated long term desensitized $(\alpha4\beta2)_2\alpha4$. Co-application of DHβE with Br-PBTC blocked reactivation of nicotine desensitized $(\alpha4\beta2)_2\alpha4$ nAChRs by Br-PBTC (*gray*). *B*, Br-PBTC (4 μM) did not reactivate long term desensitized $(\alpha4\beta2)_2\beta2$ efficaciously. *C*, effects on desensitized nAChRs by various concentrations of Br-PBTC. Nicotine (0.5 μM) was incubated with nAChRs for 6 h before acute application of Br-PBTC. The evoked responses by Br-PBTC were normalized to maximum ACh responses of nAChRs. Br-PBTC greatly reactivated long term desensitized $(\alpha4\beta2)_2\alpha4$ nAChRs but showed very little effect on $(\alpha4\beta2)_2\beta2$ nAChRs. Results are the mean ± S.E. (*error bars*).

The maximum reactivation efficacy of Br-PBTC relative to maximal ACh responses is 92.5 ± 2.7% for $(\alpha4\beta2)_2\alpha4$ but only 27.6 ± 6.5% for $(\alpha4\beta2)_2\beta2$. These data suggest that Br-PBTC reactivates long term desensitized $(\alpha4\beta2)_2\alpha4$ nAChRs more efficiently. Thus both activation and reactivation are more efficient with three ACh binding sites. This potentiation of Br-PBTC is specific to agonist-desensitized nAChRs. Br-PBTC could not reactivate antagonist-inactivated nAChRs (*green traces* in Fig. 9).

Competitive Antagonists Block Potentiation by Br-PBTC—Competitive antagonists block activation by agonists because they bind to the same sites as agonists but do not activate nAChRs. We investigated whether competitive antagonists affect potentiation of the allosteric ligand Br-BPTC. One of the important native nAChR subtypes that contain only one potential Br-PBTC site is $(\alpha6\beta2)(\alpha4\beta2)\beta3$ (33). This is the subtype that regulates nicotine addiction because knock-out of α4, α6, or β2 abolished nicotine self-administration in rodents (34). Br-PBTC did not potentiate activation of $(\alpha6\beta2)_2\beta3$ expressed in oocytes (data not shown), but it increased ACh (3 μM) activation of $(\alpha6\beta2)(\alpha4\beta2)\beta3$ by 99.0 ± 13.6% (representative kinetics shown in Fig. 10*A*). This is consistent with the finding in Fig. 5 that only one α4 subunit is required for Br-PBTC potentiation. One feature of $(\alpha6\beta2)(\alpha4\beta2)\beta3$ is that the competitive antagonist α-conotoxin MII selectively blocks its activation from the α6/β2 interface. This antagonist site is far away from the α4 C-tail where Br-PBTC acts. α-Conotoxin MII (50 nM) completely blocked activation by ACh and potentiation by Br-PBTC (Fig. 10*B*). This is consistent with the idea that activation is a cooperative event involving conformational change in the whole nAChR, and antagonist inhibition of any one ACh site is sufficient to prevent activation (35, 36). Blockage by competitive antagonists also applies to potentiation of Br-PBTC on other α4* nAChRs. The competitive antagonist DHβE selective for β2 nAChRs blocked activation of HEK cell lines expressing $(\alpha4\beta2)_2\beta2$ and $(\alpha4\beta2)_2\alpha4$ nAChRs in the presence of Br-PBTC (Fig. 11). DHβE also inhibited reactivation of both short term and long term desensitized nAChRs by Br-PBTC (*gray traces* in Figs. 8 and 9).

Discussion

Developing subtype-selective therapeutics is challenging for nAChRs. Efforts have been made to develop allosteric modulators binding to non-conserved regions to achieve subtype selectivity (6, 7). Only the human α2 and α4 subunits share similar sequences at the C-tail. Other human subunits differ in length and the amino acid sequences in this region. This makes the C-tail a promising target for selective PAMs. Here we showed that, besides steroids, non-steroid structures could act from the α4 C-tail as PAMs and exhibit submicromolar affinity. Engineering the α4 C-tail onto β2 subunits enabled estrogens to potentiate through this mutant β2 subunit (15). A suitable

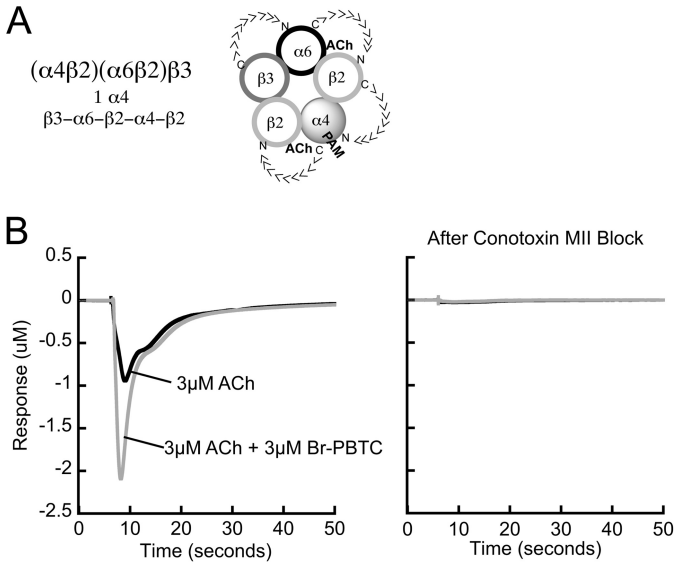

FIGURE 10. **Effect of Br-PBTC and α-conotoxin MII on (α4β2)(α6β2)β3 nAChRs expressed in oocytes.** *A*, illustration of expressing (α4β2)(α6β2)β3 from a pentameric concatemer. These nAChRs have only one C-tail PAM site for Br-PBTC. It is part of a concatemer linking α4 with β2. B, acting through the single α4 subunit, Br-PBTC potentiated activation of (α4β2)(α6β2)β3 by ACh. Acting through the single α6β2 ACh binding site, antagonism by 50 nM conotoxin MII blocked both activation and potentiation. Responses to ACh (3 μM) are shown in *black*, and responses to ACh with Br-PBTC (3 μM) are shown in *gray*.

PAM to bind the C-tail of β2 and interact with the end of its M4 might produce a β2-selective effect. Perhaps in this way PAMs could be found that would be selective for any subunit. These ligands might behave similarly to type II PAMs like Br-PBTC, but they might also be negative allosteric modulators or allosteric agonists, depending on their structures. There is not clear guidance for how to design or select such ligands, but 17β-estradiol and Br-PBTC illustrate examples of structurally different compounds with similar PAM properties. Suitable selection approaches using stoichiometry-specific nAChR cell lines might allow for the discovery of PAMs, negative allosteric modulators, and allosteric agonists for many nAChR subunits that would be useful tools for studying nAChRs and as drugs both *in vitro* and *in vivo*.

The C-tail PAM site is stereoselective. Neither the enantiomer of Br-PBTC[5] nor estrogens (14) potentiate α4* nAChRs. Stereoselectivity suggests that the PAM and the C-tail of the α4 subunit interact with protein rather than membrane lipid. PAM bound to the short α4 C-tail must interact stereospecifically with a nearby region, probably on the same subunit, which is capable of influencing the channel gate. There are prolines at the extracellular end of the M4 transmembrane domains. These prolines may contribute to a stereoselective site that interacts with the PAM bound to the C-tail to mediate the PAM effects. Several other important subunit structural elements are close to this stereoselective site: the end of β10 strand to M1, the cys-loop, M2-M3 loop, β1-β2 loop, and β8-β9 loop. Movement of these structural elements contributes to passing the conformational changes from binding of the agonist in the extracellular domain to opening of the transmembrane channel pore (37, 38). Ivermectin, a compound acting directly on these structural elements, is a PAM on α7 (6) and an allosteric agonist on glutamate-gated chloride channels where its binding site has been localized in receptor crystals near this region (38). A lipid molecule binds competitively to the same region as ivermectin (39). Both ivermectin and this lipid induce channel pore opening but through slightly different conformation changes. These suggest that the transmembrane domains are quite flexible. The subtleties involved in channel opening are small (39); thus, pulling or pushing a bit on the extracellular end of M4 might be enough to mediate action of a PAM.

Although Br-PBTC acts from α subunits, β subunits also play a role. Br-PBTC has greater effects on nAChRs with β2 subunits over those with β4 subunits (Fig. 2). It is not clear whether this is because of the greater sensitivity to activation of β2* nAChRs or because β subunits directly contribute to the Br-PBTC PAM effect.

It is not evident how a PAM binding to an α4 C-tail affects activation or desensitization. Estrogens do not potentiate α4 subunits whose C-terminal end is linked into another subunit such as the concatemer α4-β2 (29). However, Br-PBTC potentiated the C-tail-linked α4 subunit equally efficiently as the free subunit (Figs. 5 and 6). This allowed us to express various concatemers with a free α3 subunit to reduce binding sites for Br-PBTC (Fig. 6). We cannot rule out the possibility that Br-BPTC can bind to the α3 C-tail but cannot potentiate nAChR activation. Occupancy by agonists affects nAChR activation and desensitization (11, 12). Using an α3 subunit to replace α4 maintained the number of agonist sites among nAChRs. Therefore, Br-PBTC is a better tool than estrogens to study the relationship between occupancy and potentiation of PAMs acting at the C-tail. Moreover, given the activity of estrogens at nuclear receptors, Br-PBTC would be a better ligand to study effects of nAChRs *in vivo*. That Br-PBTC potentiated linked α4 C-tails in concatemers indicates that a free tip of the C-tail is not required for potentiation from this site. The linker in the α4-β2 concatemer might have prevented the entrance of estrogens into the C-tail site.

A previous study used concatemers to achieve different numbers of α4 subunits with free C-tails and showed that more α4 subunits increased potentiation efficacy by estrogens (15). Using Br-PBTC, we confirmed and extended this C-tail potentiation mechanism. Upon agonist binding, nAChRs go through various conformational changes from the resting state (*R*) to the open state (*O*) and or desensitized state (*D*) (Fig. 12*A*). There are different types of desensitized states (6, 40, 41). Some have lower energy barriers and are favored soon after ligand binding, *i.e.* short term desensitization (D_S). Some have lower energy levels and are preferred after long term incubation with agonists (D_L). When an antagonist binds, nAChRs go into an inactive state (*I*) or are forced to remain in a resting state that prevents activation. When a PAM binds to the C-tail of α4, it increases the probability of channel opening (42). The increase of channel open probability only requires one C-tail site, and its extent is proportionate to the number of C-tail PAM sites in a nAChR (Figs. 6*B* and 12*B*) (15). PAMs reactivate short term desensitized nAChRs from the C-tail also in an occupancy-de-

[5] Z. Jin, J. Wang, J. Lindstrom, P. J. Kenny, and T. M. Kamenecka, unpublished observations.

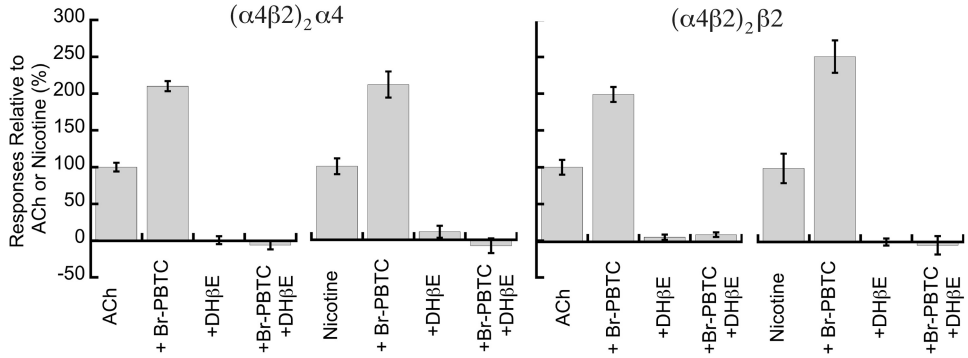

FIGURE 11. **The competitive antagonist DhβE blocks Br-PBTC potentiated activation.** HEK cell lines expressing fixed $(\alpha4\beta2)_2\alpha4$ or $(\alpha4\beta2)_2\beta2$ stoichiometries were used. Br-PBTC (3 μM) was pre-applied to cells for 15 min before application of agonists with or without DHβE (1 μM). Peak responses were normalized to evoked responses by an agonist alone. Medium concentration of an agonist was used: for $(\alpha4\beta2)_2\alpha4$, 4 μM ACh or 0.4 μM nicotine; for $(\alpha4\beta2)_2\beta2$, 0.4 μM ACh or 0.1 μM nicotine. Results are the mean ± S.E. (*error bars*).

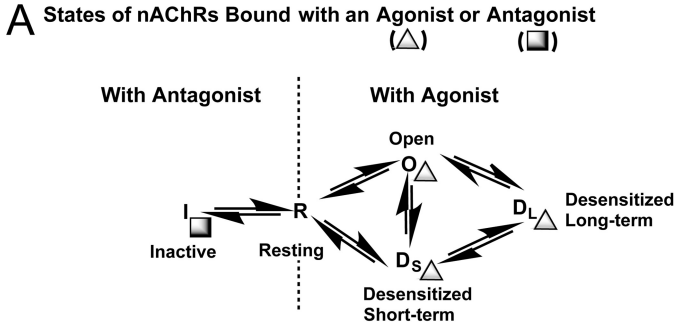

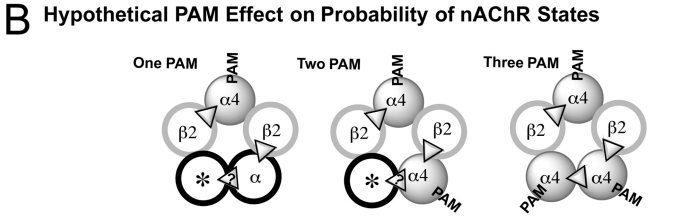

nAChR States	Number of PAM sites 1	2	3
O	+	++	+++
D_S	0	-	- -
D_L	0	0	-
I	0	0	0

FIGURE 12. **Proposed potentiation mechanism for C-tail PAMs.** *A*, states of nAChRs bound with an agonist or antagonist. Upon agonist binding, nAChRs go through various conformation changes from the resting state (*R*) to the open state (*O*) and non-conductive short term (D_S) or long term (D_L) desensitized states. When an antagonist binds to nAChRs, nAChRs go into an inactive state (*I*) or is held in a resting state that prevents further activation by agonists. nAChRs may pass through various transitional states, which are not displayed in the figure. *B*, hypothetical PAM effects on probability of nAChR states. * indicates that the position can be occupied either by an α or a β subunit. An agonist site can form at the α/α and α/β subunit interface but not the β/α subunit interface. Therefore, a question mark for agonist binding is annotated at those undefined interfaces. Higher PAM occupancy increases the probability of nAChRs being in the open state and decreases the probability in the D_S or D_L states. Therefore, α4-selective PAMs showed the greatest potentiation effect on $(\alpha4\beta2)_2\alpha4$ nAChRs with three α4 subunits.

pendent manner but require occupying two or more C-tail sites (Figs. 7). This suggests that Br-PBTC increases exit rates from the D_S state to the O state, thus destabilizing the D_S state (Fig. 12*B*). Occupying three C-tail sites is required to efficiently reactivate long term desensitized nAChRs (Figs. 9 and 11*B*). The D_L state is favored over time because it has the lowest energy level. Br-PBTC likely needs to bind to three α4 subunits to initiate sufficient conformational change to compensate for the energy loss from leaving the D_L state. The cooperative effect of Br-PBTC binding to three sites also enables Br-PBTC to increase agonist sensitivity of $(\alpha4\beta2)_2\alpha4$ nAChRs. PAMs at the α4 C-tail cannot activate antagonist-bound nAChRs, and antagonists block their potentiation (Figs. 8–11). This is consistent with the concerted conformational change model for activation, *i.e.* any one ACh site being held in a resting conformation through an antagonist blocking closing of its C-loop prevents activation (43).

α4β2* nAChRs are the most prevalent subtypes in brain (44). PAMs promoting activation of these nAChRs could be beneficial in improving cognition, movement, learning, and memory and reducing pain or aggressive behaviors, thus beneficial for analgesia, autism, Parkinson, or Alzheimer diseases (2, 3, 7, 45, 46). α4β2* PAMs are also promising in treating nicotine addiction. Sustained levels of nicotine, which usually keep high affinity nAChRs desensitized, are found in chronic smokers (32). An α4β2 type II PAM, desformylflustrabromine (dFBr), reduced nicotine self-administration in rats (47). dFBr potentiates nAChR functions through binding to the principal face of β2 subunits homologous to the ACh site at the principal face of α subunits (48). This is similar to how morantel potentiates α3β2 nAChRs (49) but different from Br-PBTC. Although differing in binding, Br-PBTC may also benefit smokers like desformylflustrabromine because potentiation of $(\alpha6\beta2)(\alpha4\beta2)\beta3$ nAChRs might achieve sufficient reward from lower concentrations of nicotine (34) and because potentiation of $(\alpha4\beta2)_2\alpha5$ nAChRs might increase aversion to high concentrations of nicotine (50).

The unique potentiation profile of Br-PBTC makes it a good research tool for differentiating nAChR subtypes. The nAChR subtype expression pattern differs between brain areas (5, 33). The α6-selective antagonist α-conotoxin MII helps distinguish α6 and non-α6 nAChRs. Br-PBTC selectively potentiates α6α4* nAChRs. This differentiates them from α6(nonα4) nAChRs. In combination with α-conotoxin MII, Br-PBTC can further distinguish α4α6* from α4(nonα6) nAChRs. Because

Br-PBTC selectively reactivates long term desensitized $(\alpha4\beta2)_2\alpha4$ nAChRs, it can be used *in vivo* to distinguish this subtype from other nAChR subtypes, such as $(\alpha4\beta2)_2\alpha5$, $(\alpha4\beta2)_2\beta2$, $(\alpha4\beta2)_2\beta3$ etc.

In summary, using the novel type II PAM Br-PBTC, we learned more about potentiation from the C-tail PAM site. We found that activation and reactivation increase with higher PAM occupancy at the C-tail site. It remains to be determined *in vivo* how chronic exposure to ACh or agonist drugs in the presence of Br-PBTC will influence smoldering activation of nAChRs largely desensitized by agonists. It also remains to be determined how ligands bound to the α4 C-tail interact with the channel to influence its opening, whether negative allosteric modulators or allosteric agonists can act from this site, whether similar sites can be found on other subunits, and whether ligands for them will prove to be useful drugs.

Author Contributions—J. W. and J. L. designed the study and wrote the paper. J. W. and A. K. designed and constructed plasmids and cell lines. J. W. and J. N. performed the FlexStation and electrophysiology assays. Z. J. and T. M. K. provided the chemical tools. P. J. K. contributed to discussions of the *in vivo* use of the PAM. P. J. K., J. L., and T. M. K. acquired funding to support this study. All authors analyzed data, revised, and approved the final version of the manuscript.

Acknowledgments—We thank Dr. Julian R. A. Wooltorton for advice on Fig. 12. We thank Aarati Sriram for technical assistance.

References

1. De Biasi, M., and Dani, J. A. (2011) Reward, addiction, withdrawal to nicotine. *Annu. Rev. Neurosci.* **34,** 105–130
2. Lewis, A. S., and Picciotto, M. R. (2013) High-affinity nicotinic acetylcholine receptor expression and trafficking abnormalities in psychiatric illness. *Psychopharmacology* **229,** 477–485
3. Picciotto, M. R., Lewis, A. S., van Schalkwyk, G. I., and Mineur, Y. S. (2015) Mood and anxiety regulation by nicotinic acetylcholine receptors: a potential pathway to modulate aggression and related behavioral states. *Neuropharmacology* **96,** 235–243
4. Hurst R., Rollema H., and Bertrand D. (2013) Nicotinic acetylcholine receptors: from basic science to therapeutics. *Pharmacol. Ther.* **137,** 22–54
5. Zoli, M., Pistillo, F., and Gotti, C. (2015) Diversity of native nicotinic receptor subtypes in mammalian brain. *Neuropharmacology* **96,** 302–311
6. Williams, D. K., Wang, J., and Papke, R. L. (2011) Positive allosteric modulators as an approach to nicotinic acetylcholine receptor-targeted therapeutics: advantages and limitations. *Biochem. Pharmacol.* **82,** 915–930
7. Grupe, M., Grunnet, M., Bastlund, J. F., and Jensen, A. A. (2015) Targeting α4β2 nicotinic acetylcholine receptors in central nervous system disorders: perspectives on positive allosteric modulation as a therapeutic approach. *Basic Clin. Pharmacol. Toxicol.* **116,** 187–200
8. Gill, J. K., Savolainen, M., Young, G. T., Zwart, R., Sher, E., and Millar, N. S. (2011) Agonist activation of α7 nicotinic acetylcholine receptors via an allosteric transmembrane site. *Proc. Natl. Acad. Sci. U.S.A.* **108,** 5867–5872
9. Grønlien, J. H., Håkerud, M., Ween, H., Thorin-Hagene, K., Briggs, C. A., Gopalakrishnan, M., and Malysz, J. (2007) Distinct profiles of α7 nAChR positive allosteric modulation revealed by structurally diverse chemotypes. *Mol. Pharmacol.* **72,** 715–724
10. Gill-Thind, J. K., Dhankher, P., D'Oyley, J. M., Sheppard, T. D., and Millar, N. S. (2015) Structurally similar allosteric modulators of α7 nicotinic acetylcholine receptors exhibit five distinct pharmacological effects. *J. Biol. Chem.* **290,** 3552–3562
11. Benallegue, N., Mazzaferro, S., Alcaino, C., and Bermudez, I. (2013) The additional ACh binding site at the α4(+)/α4(−) interface of the $(\alpha4\beta2)_2\alpha4$ nicotinic ACh receptor contributes to desensitization. *Br. J. Pharmacol.* **170,** 304–316
12. Rayes, D., De Rosa, M. J., Sine, S. M., and Bouzat, C. (2009) Number and locations of agonist binding sites required to activate homomeric Cys-loop receptors. *J. Neurosci.* **29,** 6022–6032
13. Wang, J., Kuryatov, A., Sriram, A., Jin, Z., Kamenecka, T. M., Kenny, P. J., and Lindstrom, J. (2015) An accessory agonist binding site promotes activation of α4β2* nicotinic acetylcholine receptors. *J. Biol. Chem.* **290,** 13907–13918
14. Paradiso, K., Zhang, J., and Steinbach, J. H. (2001) The C terminus of the human nicotinic α4β2 receptor forms a binding site required for potentiation by an estrogenic steroid. *J. Neurosci.* **21,** 6561–6568
15. Jin, X., and Steinbach, J. H. (2011) A portable site: a binding element for 17β-estradiol can be placed on any subunit of a nicotinic α4β2 receptor. *J. Neurosci.* **31,** 5045–5054
16. Wang, F., Gerzanich, V., Wells, G. B., Anand, R., Peng, X., Keyser, K., and Lindstrom, J. (1996) Assembly of human neuronal nicotinic receptor α5 subunits with α3, β2, and β4 subunits. *J. Biol. Chem.* **271,** 17656–17665
17. Wang, F., Nelson, M. E., Kuryatov, A., Olale, F., Cooper, J., Keyser, K., and Lindstrom, J. (1998) Chronic nicotine treatment up-regulates human α3β2 but not α3β4 acetylcholine receptors stably transfected in human embryonic kidney cells. *J. Biol. Chem.* **273,** 28721–28732
18. Gerzanich, V., Kuryatov, A., Anand, R., and Lindstrom, J. (1997) "Orphan" α6 nicotinic AChR subunit can form a functional heteromeric acetylcholine receptor. *Mol. Pharmacol.* **51,** 320–327
19. Kuryatov, A., Gerzanich, V., Nelson, M., Olale, F., and Lindstrom, J. (1997) Mutation causing autosomal dominant nocturnal frontal lobe epilepsy alters Ca^{2+} permeability, conductance, and gating of human α4β2 nicotinic acetylcholine receptors. *J. Neurosci.* **17,** 9035–9047
20. Ley, C. K., Kuryatov, A., Wang, J., and Lindstrom, J. M. (2014) Efficient expression of functional $(\alpha6\beta2)_2\beta3$ AChRs in *Xenopus* oocytes from free subunits using slightly modified α6 subunits. *PLoS ONE* **9,** e103244
21. Kuryatov, A., Olale, F. A., Choi, C., and Lindstrom, J. (2000) Acetylcholine receptor extracellular domain determines sensitivity to nicotine-induced inactivation. *Eur. J. Pharmacol.* **393,** 11–21
22. Kuryatov, A., Berrettini, W., and Lindstrom, J. (2011) Acetylcholine receptor (AChR) α5 subunit variant associated with risk for nicotine dependence and lung cancer reduces $(\alpha4\beta2)_2\alpha5$ AChR function. *Mol. Pharmacol.* **79,** 119–125
23. Kuryatov, A., and Lindstrom, J. (2011) Expression of functional human α6β2β3* AChRs in *Xenopus* oocytes achieved through subunit chimeras and concatemers. *Mol. Pharmacol.* **79,** 126–140
24. Nelson, M. E., Kuryatov, A., Choi, C. H., Zhou, Y., and Lindstrom, J. (2003) Alternate stoichiometries of α4β2 nicotinic acetylcholine receptors. *Mol. Pharmacol.* **63,** 332–341
25. Kuryatov, A., Luo, J., Cooper, J., and Lindstrom, J. (2005) Nicotine acts as a pharmacological chaperone to up-regulate human α4β2 acetylcholine receptors. *Mol. Pharmacol.* **68,** 1839–1851
26. Weltzin, M. M., and Schulte, M. K. (2010) Pharmacological characterization of the allosteric modulator desformylflustrabromine and its interaction with α4β2 neuronal nicotinic acetylcholine receptor orthosteric ligands. *J. Pharmacol. Exp. Ther.* **334,** 917–926
27. Mazzaferro, S., Benallegue, N., Carbone, A., Gasparri, F., Vijayan, R., Biggin, P. C., Moroni, M., and Bermudez, I. (2011) Additional acetylcholine (ACh) binding site at α4/α4 interface of $(\alpha4\beta2)_2\alpha4$ nicotinic receptor influences agonist sensitivity. *J. Biol. Chem.* **286,** 31043–31054
28. Harpsøe, K., Ahring, P. K., Christensen, J. K., Jensen, M. L., Peters, D., and Balle, T. (2011) Unraveling the high- and low-sensitivity agonist responses of nicotinic acetylcholine receptors. *J. Neurosci.* **31,** 10759–10766
29. Zhou, Y., Nelson, M. E., Kuryatov, A., Choi, C., Cooper, J., and Lindstrom, J. (2003) Human α4β2 acetylcholine receptors formed from linked subunits. *J. Neurosci.* **23,** 9004–9015
30. Krashia, P., Moroni, M., Broadbent, S., Hofmann, G., Kracun, S., Beato, M., Groot-Kormelink, P. J., and Sivilotti, L. G., (2010) Human α3β4 neuronal nicotinic receptors show different stoichiometry if they are expressed in *Xenopus* oocytes or mammalian HEK293 cells. *PLoS ONE* **5,** e13611
31. Jin, X., Bermudez, I., Steinbach, J. H. (2014) The nicotinic α5 subunit can replace either an acetylcholine-binding or nonbinding subunit in the

α4β2* neuronal nicotinic receptor. *Mol. Pharmacol.* **85,** 11–17
32. Picciotto, M. R., Addy, N. A., Mineur, Y. S., and Brunzell, D. H. (2008) It's not "either/or": activation and desensitization of nicotinic acetylcholine receptors both contribute to behaviors related to nicotine addiction and mood. *Prog. Neurobiol.* **84,** 329–342
33. Wang, J., Kuryatov, A., and Lindstrom, J. (2015) Expression of cloned α6* nicotinic acetylcholine receptors. *Neuropharmacology* **96,** 194–204
34. Pons, S., Fattore, L., Cossu, G., Tolu, S., Porcu, E., McIntosh, J. M., Changeux, J. P., Maskos, U., and Fratta, W. (2008) Crucial role of α4 and α6 nicotinic acetylcholine receptor subunits from ventral tegmental area in systematic nicotinic self- administration. *J. Neurosci.* **28,** 12318–12327
35. Unwin, N., and Fujiyoshi, Y. (2012) Gating movement of acetylcholine receptor caught by plunge-freezing. *J. Mol. Biol.* **422,** 617–634
36. Fletcher, G. H., and Steinbach, J. H. (1996) Ability of nondepolarizing neuromuscular blocking drugs to act as partial agonists at fetal and adult mouse muscle nicotinic receptors. *Mol. Pharmacol.* **49,** 938–947
37. Lee, W. Y., and Sine, S. M. (2005) Principal pathway coupling agonist binding to channel gating in nicotinic receptors. *Nature* **438,** 243–247
38. Hibbs, R. E., and Gouaux, E. (2011) Principles of activation and permeation in an anion-selective Cys-loop receptor. *Nature* **474,** 54–60
39. Althoff, T., Hibbs, R. E., Banerjee, S., and Gouaux, E. (2014) x-ray structures of GluCl in apo states reveal a gating mechanism of Cys-loop receptors. *Nature* **512,** 333–337
40. Boyd, N. D. (1987) Two distinct kinetic phases of desensitization of acetylcholine receptors of clonal rat PC12 cells. *J. Physiol.* **389,** 45–67
41. Yu, K. D., Liu, Q., Wu, J., and Lukas, R. J. (2009) Kinetics of desensitization and recovery from desensitization for human α4β2-nicotinic acetylcholine receptors stably expressed in SH-EP1 cells. *Acta Pharmacol. Sin.* **30,** 805–817
42. Curtis, L., Buisson, B., Bertrand, S., and Bertrand, D. (2002) Potentiation of human α4β2 neuronal nicotinic acetylcholine receptor by estradiol. *Mol. Pharmacol.* **61,** 127–135
43. Changeux, J. P. (2013) 50 years of allosteric interactions: the twists and turns of the models. *Nat. Rev. Mol. Cell Biol.* **14,** 819–829
44. Gaimarri, A., Moretti, M., Riganti, L., Zanardi, A., Clementi, F., and Gotti, C. (2007) Regulation of neuronal nicotinic receptor traffic and expression. *Brain Res. Rev.* **55,** 134–143
45. Srinivasan, R., Henderson, B. J., Lester, H. A., and Richards, C. I. (2014) Pharmacological chaperoning of nAChRs: a therapeutic target for Parkinson's disease. *Pharmacol. Res.* **83,** 20–29
46. Dineley, K. T., Pandya, A. A., and Yakel, J. L. (2015) Nicotinic ACh receptors as therapeutic targets in CNS disorders. *Trends Pharmacol. Sci.* **36,** 96–108
47. Liu, X. (2013) Positive allosteric modulation of α4β2 nicotinic acetylcholine receptors as a new approach to smoking reduction: evidence from a rat model of nicotine self-administration. *Psychopharmacology* **230,** 203–213
48. Weltzin, M. M., and Schulte, M. K. (2015) Desformylflustrabromine modulates α4β2 nAChR high- and low- sensitivity isoforms at allosteric clefts containing the β2 subunit. *J. Pharmacol. Exp. Ther.* **354,** 184–194
49. Seo, S., Henry, J. T., Lewis, A. H., Wang, N., and Levandoski, M. M. (2009) The positive allosteric modulator morantel binds at noncanonical subunit interfaces of neuronal nicotinic acetylcholine receptors. *J. Neurosci.* **29,** 8734–8742
50. Fowler C. D., Lu, Q., Johnson, P. M., Marks, M. J., and Kenny, P. J. (2011) Habenular α5 nicotinic receptor subunit signalling controls nicotine intake. *Nature* **471,** 597–601

Neurobiology:

A Novel α2/α4 Subtype-selective Positive Allosteric Modulator of Nicotinic Acetylcholine Receptors Acting from the C-tail of an α Subunit

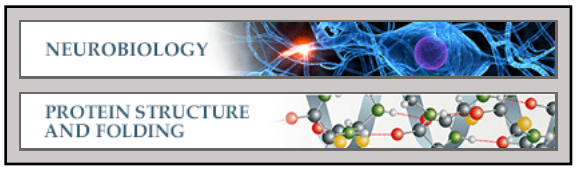

Jingyi Wang, Alexander Kuryatov, Zhuang Jin, Jack Norleans, Theodore M. Kamenecka, Paul J. Kenny and Jon Lindstrom

J. Biol. Chem. 2015, 290:28834-28846.
doi: 10.1074/jbc.M115.676551 originally published online October 2, 2015